MECHANICAL PROPERTIES OF MARBLE WITH DIFFERENT JOINT INCLINATIONS UNDER ENGINEERING DISTURBANCE

by

Chen-Di LOU[a,b], Jing XIE[b,c*], Er-Sheng ZHA[d], Ru ZHANG[a,b,c], Li REN[b], Ze-Tian ZHANG[b,c], Xiao-Ling LIU[c], and Kun XIAO[c]

[a] Institute for Disaster Management and Reconstruction, Sichuan University, Chengdu, China
[b] MOE Key Laboratory of Deep Earth Science and Engineering, Sichuan University, Chengdu, China
[c] College of Water Resources and Hydro Power, Sichuan University, Chengdu, China
[d] State Key Laboratory of Water Resource Protection and Utilization in Coal Mining, National Institute of Clean and Low Carbon Energy, Beijing, China

Original scientific paper
https://doi.org/10.2298/TSCI2305829L

This study examined the fracture morphology properties of rock cores and studied the mechanical characteristics of jointed rock at depths of 2400 m, with inclinations of 15°, 30°, and 60°. The results showed that jointed rock is significantly controlled by joint weak areas, particularly when the joint inclination exceeds 30°. Additionally, rock damage increases with joint inclination during engineering disturbance, however, its pre-peak plastic characteristics weaken with joint inclination. The damage stress level is higher with a larger joint inclination, decreasing the bearing capacity. Further, a strength criterion for jointed rock considering engineering disturbance was established. It is found that strength exhibits a V-shaped distribution with joint inclination, and 30° to 75° jointed rock is significantly lower than before the disturbance.

Key words: *deep rock, engineering disturbance, single fracture roughness, jointed damage, strength criterion*

Introduction

With the diminishing availability of shallow resources and space, underground engineering is gradually developing towards the deep [1]. However, deep environment increases stress levels of surrounding rock, leading to fully developed fracture networks and reduced bearing capacity after engineering disturbance, which brought significant challenges for deep engineering projects.

Natural rock masses typically have numerous fractures that affect their mechanical properties. Uniaxial compression experiments show significant anisotropy in the influence of joint spacing on strength and deformation [2-4], while triaxial compression experiments indicate that joint geometry and confining pressure affect mechanical properties and failure modes [5]. Joint inclination angle controls the failure mode of jointed rock masses under low confining pressure, with joint arrangement having a greater impact on deformation and strength behavior than confining pressure [6, 7]. The stability of surrounding rock is determined by lithology,

* Corresponding author, e-mail: xiejing200655@163.com

structural plane, and in-situ stress, with most instability failure resulting from crack propagation in internal joints due to disturbance stress such as excavation and mining [8]. In deep high stress concentrations, disturbances may change the internal structure of rock masses, weakening bearing capacity and inducing macroscopic failure.

Previous research has focused on jointed rock mass structure and mechanical properties, but ignored time-dependent changes under high stress conditions. Engineering disturbances affect stress distribution and concentration in fractured rock masses. Therefore, this study extracts effective fracture roughness from on-site rock core structural surfaces and conducts mechanical behavior tests with different joint inclination angles at 2400 m to reveal strength and deformation characteristics.

Experiment

Sampling and preparation

This experiment utilized fine-crystalline marble core samples from the Baishan Formation of the China Jinping Underground Laboratory located 2400 m beneath the surface of Jinping Mountain, Sichuan province, China. The core samples were constructed according to ISRM recommendations [9] and had a diameter of 50 mm and a height of 100 mm. The fracture morphology of the 13th on-site core segment was quantitatively evaluated using the box-counting method [10] and showed an average fractal dimension of 1.027 for single fractures. The fracture scattered point co-ordinates were then reconstructed and rotated at angles of 15°, 30°, and 60° to obtain samples through program-controlled cutting methods, as shown in fig. 1.

Procedures

Excavation may cause deformation and stress redistribution in surrounding rock mass. Stress evolution around the chamber during cavern excavation can be divided into in-situ stress stage, excavation disturbance stage, and stress stability stage, as shown in fig. 2 [11], wherein, λ represents the lateral pressure coefficient, γ is the bulk density of overlying strata, and H represents occurrence depth. According to field measurement results [12], the loading path at 2400 m follows the axial stress sequence of 76.3 MPa → 114.5 MPa → 229.0 MPa → 165.4 MPa, and the confining pressure sequence is 63.6 MPa → 57.2 MPa → 25.4 MPa → 19.5 MPa, accomplished by the MTS 815 rock mechanics test system of Sichuan University. Confining pressure was to be loaded first, followed by axial pressure before Point ① and then both the axial and confining pressures were adjusted simultaneously. Once reaching Point ④, the confining pressure would be maintained and axial compression would continuous.

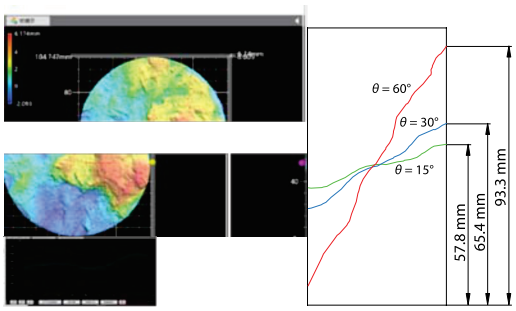

Figure 1. Fracture scanning and sample preparation

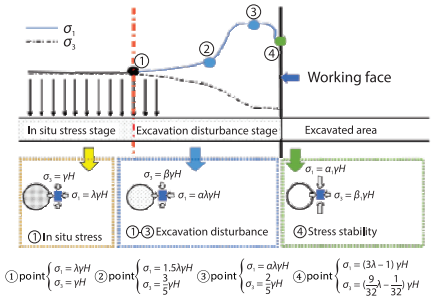

Figure 2. Excavation disturbance influence on stress state of surrounding rock [11]

Results and analysis

Stress evolution of marble during disturbance

Stress-strain curve characteristics

Figure 3 shows the stress-strain curves of marble during engineering disturbance. Both axial and circumferential strains of marble continue to increase during the middle stage of engineering disturbance, with dilatancy behavior occurring near Point ② stress state. Generally, the volumetric strain reaches its peak value before Point ③, transitioning from contraction expansion and continuing to expand thereafter. At maximum axial stress, Point ③, axial strain of 15° and 30° jointed rock is 1.10 and 1.18 times that of intact rock, and circumferential strain is 1.23 and 1.26 times. A greater angle between joint direction and principal axis results in greater deformation. The stress level at the peak point reduces with an increase in joint inclination. Meanwhile, for 60° jointed rock, the maximum volumetric strain is reached after Point ②, with rapid expansion leading to failure before Point ③. During the stress adjustment unloading stage, the axial strain of rock rebounds as axial stress unloads, while circumferential and volumetric strains continue to expand. At this point, the rock has accumulated some plastic deformation, which increases with joint inclination, and non-linear characteristics become more prominent. Overall, it is evident that the mechanical characteristics of rock significantly impact its internal joint inclination, and deep engineering disturbance may cause damage that depends on the joint structure of rock mass.

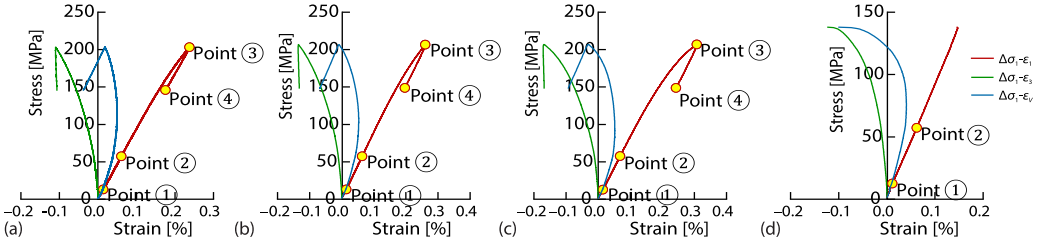

Figure 3. Stress-strain curve during disturbance; (a) intact rock, (b) 15° jointed rock, (c) 30° jointed rock, and (d) 60° jointed rock

Deformation characteristics

During disturbance, rock undergoes a complex loading and unloading stress environment. Fractured rock masses can be considered an equivalent continuous medium at macroscopic mechanical behavior level. The equivalent deformation modulus of rock can be expressed:

$$\tilde{E} = \frac{\left(\Delta\sigma_1 + 2\Delta\sigma_3\right)\left(\Delta\sigma_1 - \Delta\sigma_3\right)}{\Delta\sigma_3\left(\Delta\varepsilon_1 - 2\Delta\varepsilon_3\right) + \Delta\sigma_1\Delta\varepsilon_1} \tag{1}$$

where $\Delta\sigma_1$ is the axial stress variation, $\Delta\sigma_3$ – the lateral stress variation, $\Delta\varepsilon_1$ – the axial strain variation, and $\Delta\varepsilon_3$ – the lateral strain variation.

Table 1 displays the equivalent deformation of jointed marble, with intact rock having the highest deformation modulus, followed by 15° jointed rock and 30° jointed rock at each stress state point. This confirms that the rock's deformation resistance weakens under identical disturbance stress as joint inclination increases. At 2400 m, due to high initial geo-stress, there is only a slight variation in deformation modulus during the initial stage of engineering disturbance. However, as excavation progresses, the deformation modulus of jointed rock increases while the initial deformation modulus of intact rock remains higher but declines slightly. When

axial stress reaches its peak, Point ③, the rock's deformation resistance decreases, with 30° jointed rock demonstrating the most significant reduction (19.57%). For 60° jointed rock, natural geo-stress has already compacted internal pores, resulting in a relatively higher initial deformation modulus. Under further pressure, the rock exhibits elastic-viscous body characteristics, similar to soft rock.

Table 1. Equivalent deformation modulus of jointed marble at 2400 m

θ [°]	Stress state [MPa]			
	Point ①	Point ②	Point ③	Point ④
None	84.14	82.46	75.41	102.02
15°	75.48	77.88	70.14	97.32
30°	69.17	73.46	59.08	97.13
60°	92.06	75.01		

Stress evolution of marble after disturbance

Stress-strain curve characteristic

Figure 4 displays the stress-strain curve of marble at 2400 m, showing a reduction in deformation modulus and weakening of deformation resistance due to engineering disturbance. The failure process of intact marble and 15° jointed marble after engineering disturbance shows stable crack propagation, unstable crack propagation, stress peak platform stage, and post-peak stage. Deep rock mass has significant plastic deformation ability after undergoing complete engineering disturbance, as shown by the stress-strain curve not falling rapidly after the peak. However, this platform effect weakens with increased joint inclination, indicating less obvious plastic characteristics before the peak and more significant macroscopic fracture control by joint weak zones. Joint fissures significantly affect rock peak strength, with intact rock having a strength of 294 MPa after disturbance, while 15° and 30° jointed rocks decreased by approximately 11% and 34%, respectively, compared to intact rock. However, 60° jointed rock was destroyed during the disturbance process.

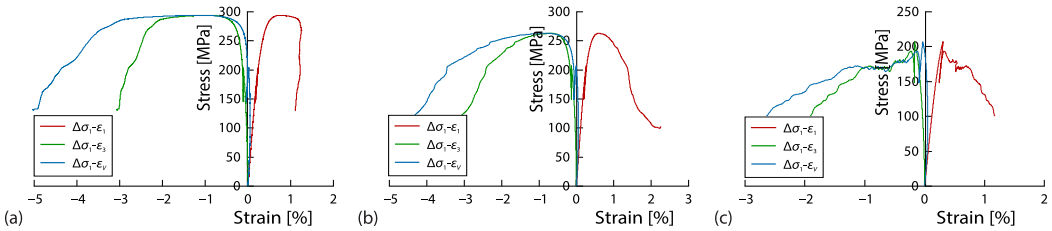

Figure 4. Stress-strain curve of marble at 2400 m; (a) intact rock, (b) 15° jointed rock, and (c) 30° jointed rock

Damage stress characteristics

The damage stress of rocks is conventionally regarded as their long-term strength indicator. During engineering disturbance, rocks may accumulate varying degrees of damage. At 2400 m, the maximum volumetric strain of marble occurs during the disturbance process. Consequently, the stress level corresponding to the rock's maximum strain value after completing the disturbance stress process is deemed its damage stress, as shown in fig. 5.

Table 2 displays the damage stress parameters of rocks at 2400 m during and after disturbance. The maximum volumetric strain of rocks appears in the stress climbing stage, Point ② → Point ③, of engineering disturbance. Due to deep high stress conditions, the maximum volumetric strain of rock remains similar. Notably, the volumetric strain after disturbance always shows expansion for deep rock, indicating that the disturbance has caused significant damage. The higher the rock joint inclination, the larger the maximum volumetric strain after engineering disturbance, the higher the rock damage stress level, and the lower the bearing capacity.

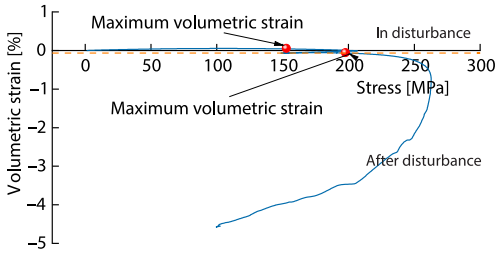

Figure 5. Determination of damage stress

Table 2. Disturbance damage stress parameters of jointed marble

θ [°]	Max volumetric strain [%]		Peak strength [MPa]	Damage stress level	Axial strain [%]	Circumferential strain [%]
	In disturbance	After disturbance				
None	0.050	–0.009	294.05	66.34%	0.230	–0.119
15°	0.053	–0.057	262.83	75.21%	0.230	–0.144
30°	0.052	–0.085	193.40	89.13%	0.272	–0.178
60°	0.041		179.10		–0.021	0.041

Deformation characteristics

Macroscopic elastic-plastic deformation and damage have occurred during engineering disturbance for deep rock masses. There is no elastic deformation of non-destructive materials in the loading process after disturbance. Thus, the transient secant modulus is used instead, which can be regarded as the equivalent deformation modulus under the damage state, and the calculation formula refers to eq. (1). Figure 6 shows the evolution of deformation modulus in marble after disturbance. The magnitude and rate of decrease in rock deformation modulus during the same deformation stage follow intact rock > 15° jointed rock > 30° jointed rock. Both the intact rock and 15° jointed rock display a downward convex shape, indicating a significant initial attenuation after disturbances. However, the 30° jointed rock presents a downward concave shape, with a decrease rate that accelerates with a higher axial strain ratio, leading to quicker loss and failure development.

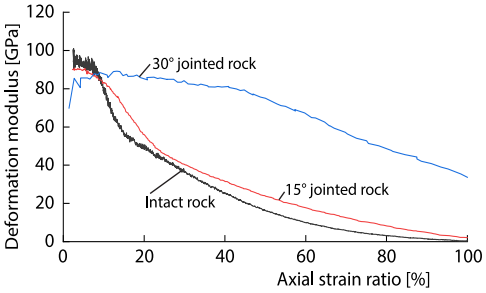

Figure 6. Deformation modulus after disturbance

Discussion

The deformation and strength properties of jointed rock depend on loading direction and structural characteristics. Therefore, micro-structure tensor coefficient, η, [13] and joint roughness coefficient, κ, were induced in the D-P criterion, which can be expressed:

$$F = \alpha\eta\kappa I_1 + \sqrt{J_2} - k = 0 \tag{2}$$

$$\eta = \eta_0 \left(1 + \Omega_{ij} l_i l_j\right) = \eta_0 \left(1 + \Omega_1 - 3\Omega_1 l_2^2\right) \tag{3}$$

$$\kappa = 1 + K_R \left(\mathrm{e}^{d-1} - 1\right) \tag{4}$$

where η_0 is the influence of the mean principal value of micro-structure tensor on the hardness of rocks, l_2 – the loading direction, the corrected value K_R is related to the joint fractal dimension d, I_1 – the first invariant of stress tensor, and J_2 – the second invariant of stress partial tensor. The parameters α and k are calculated using the DP1 criterion, which best matches the intact rock results. The DP1 criterion, the best match with the experimental results through trial calculation of intact rock, is adopted.

Based on current research [14] and calculations (α = –0.285, k = 65.958 MPa, d = 1.027, K_R = 0.5, Ω_1 = –0.35, η_0 = 0.55, κ = 1.014), the theoretical results of jointed marble strength are obtained, presented in fig. 7. The results show a V-shaped distribution pattern in rock strength as joint inclination increases, consistent with triaxial compression test results [15]. Nonetheless, deviation observed in jointed rock mass is due to engineering disturbance, resulting in the following definition of damage variable for rock caused by engineering disturbance:

$$D = \left| \frac{1 - \tilde{E}_{\varepsilon V2}}{\tilde{E}_{\varepsilon V1}} \right| \tag{5}$$

where $\tilde{E}_{\varepsilon V1}$ and $\tilde{E}_{\varepsilon V2}$ are the instantaneous deformation modulus corresponding to the maximum volumetric strain during and after disturbance, respectively. The results are shown in tab. 3.

Table 3. Damage variable parameters of marble

θ [°]	$\tilde{E}_{\varepsilon V1}$ [GPa]	$\tilde{E}_{\varepsilon V2}$ [GPa]	D
None	85.66	83.09	0.0299
15	85.23	82.18	0.0358
30	62.81	74.23	0.1817

Under high confining pressure, 90° and 0° jointed rock masses present nearly the same macroscopic strength, second only to intact rock [15]. Therefore, their damage parameters were assumed to be approximately 0.03. Polynomial fitting on the damage variable and joint inclination was performed to obtain theoretical correction, and revised results are shown in fig. 8, indicating high consistency with experiments. Notably, 30°~75° jointed rock requires particular attention in engineering practice as its bearing capacity significantly decreases below its original strength after disturbance. The minimum strength occurs between 45°~60° jointed rock, which is lower than 150 MPa, indicating such rock masses may not tolerate a complete engineering disturbance.

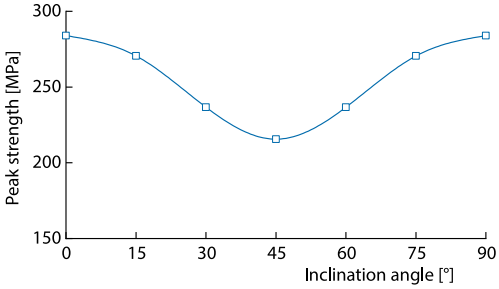

Figure 7. Theoretical results of jointed marble at 2400 m

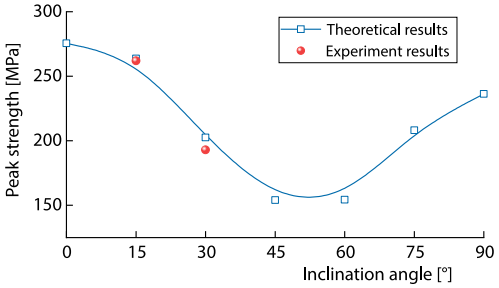

Figure 8. Theoretical results of jointed marble after disturbance at 2400 m

Conclusion

To investigate mechanical behavior of jointed rocks under engineering disturbance, a series of mechanics experiments considered disturbance stress paths was conducted. During disturbance, jointed rock accumulates plastic damage that increases with joint inclination. After disturbance, the plastic characteristics of rock under high confinement become less apparent with increasing joint inclination. The higher the joint inclination, the greater the maximum volumetric strain after engineering disturbance, the higher the damage stress level, and the lower the bearing capacity. Rock strength presents a *V*-shaped distribution pattern as joint inclination increments and 30°~75° joined rock is significantly affected by disturbance.

Acknowledgment

This work was supported by the National Natural Science Foundation of China (U1965203).

Nomenclature

D – damage variable, [–]
d – fractal dimension, [–]
$\widetilde{E}$ – equivalent deformation modulus, [GPa]
H – occurrence depth, [m]
l_2 – loading direction, [–]

Greek symbols

α_{ij} – micro-structure tensor, [–]
γ – bulk density of overlying strata, [Nm^{-3}]
θ – joint inclination, [°]
ε_V – volumetric strain, [–]
λ – lateral pressure coefficient, [–]
η – micro-structure tensor coefficient, [–]
κ – joint roughness coefficient, [–]
σ_1 – axial stress, [MPa]
σ_3 – confining pressure, [MPa]
Ω_{ij} – micro-structure tensor deviation, [–]

References

[1] Wu, S.Y., *et al*., Jinping Hydro power Project: Main Technical Issues on Engineering Geology and Rock Mechanics, *Bulletin of Engineering Geology and the Environment*, *69* (2010), 3, pp. 325-332
[2] Chen, X., *et al*., Experimental Study on Effect of Spacing and Inclination Angle of Joints on Strength and Deformation Properties of Rock Masses under Uniaxial Compression (in Chinese), *Chinese Journal of Geotechnical Engineering*, *36* (2014), 12, pp. 2236-2245
[3] Wang, J., *et al*., Analysis of Damage Evolution Characteristics of Jointed Rock Mass with Different Joint Dip Angles (in Chinese), *Journal of Harbin Institute of Technology*, *51* (2019), 8, pp. 143-150
[4] Li, J., *et al*., Experimental Study on Anisotropic Mechanical Characteristics of Jointed Rock Masses under Unloading Condition (in Chinese), *Chinese Journal of Geotechnical Engineering, 33* (2014), 2, pp. 892-900
[5] Yang, S. Q., *et al*., Experimental Investigation on Strength and Failure Behavior of Pre-cracked Marble under Conventional Triaxial Compression, *International Journal of Solids and Structures*, *45* (2008), 17, pp. 4796-4819
[6] Chen, M., *et al*., Effects of Confining Pressure on Deformation Failure Behavior of Jointed Rock, *Journal of Central South University*, *29* (2022), 4, pp. 1305-1319
[7] Huang, D., *et al*., Investigation on Mechanical Behaviors of Sandstone with Two Preexisting Flaws under Triaxial Compression, *Rock Mechanics and Rock Engineering*, *49* (2016), 2, pp. 375-399
[8] Zhong, Z., *et al*., Experimental Study on the Effects of Unloading Normal Stress on Shear Mechanical Behaviour of Sandstone Containing a Parallel Fissure Pair, *Rock Mechanics and Rock Engineering*, *53* (2020), 4, pp. 1647-1663
[9] Fairhurst, C. E., Hudson, J. A.,Draft ISRM Suggested Method for the Complete Stress-Strain Curve for Intact Rock in Uniaxial Compression, *International Journal of Rock Mechanics and Mining Sciences*, *36* (1999), 3, pp. 281-289
[10] Ai, T., *et al*., Box-Counting Methods to Directly Estimate the Fractal Dimension of a Rock Surface, *Applied Surface Science*, *314* (2014), 2, pp. 610-621
[11] Zha, E., *et al*., Long-Term Mechanical and Acoustic Emission Characteristics of Creep in Deeply Buried Jinping Marble Considering Excavation Disturbance, *International Journal of Rock Mechanics and Mining Sciences*, *139* (2021), 1, 104603

[12] Zhang, C., *et al.*, Case Histories of Four Extremely Intense Rockbursts in Deep Tunnels, *Rock Mechanics and Rock Engineering*, *45* (2012), 3, pp. 275-288
[13] Pietruszczak, S., *et al*., Modelling of Inherent Anisotropy in Sedimentary Rocks, *International Journal of Solids and Structures*, *39* (2002), 3, pp. 637-648
[14] Zhong, S. Y., *et al*., Influence of the Parameters in the Pietruszczak-Mroz Anisotropic Failure Criterion, *International Journal of Rock Mechanics and Mining Sciences*, *48* (2011), 6, pp. 1034-1037
[15] Saroglou, H., Tsiambaos, G, A modified Hoek-Brown Failure Criterion for Anisotropic Intact Rock, *International Journal of Rock Mechanics and Mining Sciences*, *45* (2008), 2, pp. 223-234

Paper submitted: March 7, 2023
Paper revised: May 12, 2023
Paper accepted: May 17, 2023